Directed percolation in asynchronous elementary cellular automata: a detailed study

Nazim A. Fatès

Directed percolation in asynchronous elementary cellular automata: a detailed study

Nazim Fatès
LORIA, University Nancy 1, Campus Scientifique B.P. 239
54 506 Vandoeuvre-lès-Nancy, France.
Nazim.Fates@loria.fr

March 23, 2007

Abstract

Cellular automata are widely used to model natural systems. Classically they are run with perfect synchrony, *i.e.*, the local rule is applied to each cell at each time step. A possible modification of the updating scheme consists in applying the rule with a fixed probability, called the synchrony rate. For some particular rules, varying the synchrony rate continuously produces a discontinuity in the behaviour of the cellular automaton. This works aims at investigating the nature of this change of behaviour using intensive numerical simulations. We apply a two-step protocol to show that the phenomenon is a phase transition whose critical exponents are in good agreement with the predicted values of directed percolation.

keywords : asynchronous cellular automata, stochastic process, discrete dynamical systems, directed percolation, phase transitions, universality class, Monte Carlo simulations, power laws

1 Introduction

1.1 General context

In half a century, research on cellular automata (CA) has progressively shifted from the study of logical properties of self-reproduction [Moo62, BCG82], to a modelling tool used to understand various "real-world systems". Most efforts focus on finding models which have the ability to reproduce observations of natural or artificial phenomena. The cellular automata paradigm, which uses discretisation of time, space and state, is obviously suited for computer simulations. However, the interpretation of the results of a simulation remains a central problem. Indeed, how to make a correspondence between "real" space and "real" time and the CA space and time? In other words, why should we trust the predictions of a CA model if the underlying hypotheses of the model are too far from reality?

This question concerns both natural and artificial systems. For some artificial systems, it may be possible to provide rather directly a good description, especially when the system modelled has natural elementary components and when it has a built-in pacemaker that governs the changes of its components. For example, classical computers and many digital electronic devices can be modelled with this approach.

However, for natural systems, it is often argued that the choice of space and time granularity introduces an implicit bias in the outcome of a simulation. For example, models based on synchronous updating may not be relevant since there is generally no clock that synchronises the components of a system. (*e.g.*, [HG93]). This argument has of course its limits and one may simply answer that a model is a simplification of reality and thus it is not supposed to perfectly mimic natural phenomena.

So the question might be better expressed in terms of a need to evaluate the robustness of a given model, *i.e.*, to evaluate to which extent a small modification of its structure will perturb its behaviour. By "modifying the structure", we mean modifying the way space and time are considered but not the rule itself.

For the cellular automata based models, as far as time is concerned, we might be interested in knowing to which extent the order of the transitions influences the outcome of a simulation (*e.g.*, [BI84, HG93]). It is sometimes argued that because the "real structure" of time is continuous, there is a zero probability of having two transitions occur simultaneously, so one may update a random single cell at each time step. This updating scheme, called the *fully asynchronous dynamics* in [FMST05], can be justified in the case of radioactive decay for example ; but there are many cases in which transitions can not be approximated by an instantaneous phenomenon, so the updating has to take into account simultaneity of transitions. Another solution is to add a probability law in each cell to determine if the update happens or not. But then we are sent back to the original problem: even if the transitions are made probabilistic, one still needs to introduce an artificial external daemon that will decide at each time step, which are the cells that will update their state.

So it seems that we are left in front of a dilemma: either to decide that cellular automata are not suitable for modelling natural phenomena or to admit that we will never know whether the properties observed in a CA simulation are produced by the transition rules, by the updating scheme or by an unknown mix of the two elements.

1.2 Robustness to asynchronism

An intermediate solution to this dilemma is to extend the study from a single model to a family of models obtained by keeping the update rule constant and varying the updating scheme [Fat04]. For example, in cellular automata, one simple way of producing such families of models is to consider the so called α-*asynchronous dynamics* [FRST06], in which each cell independently updates its state with probability α at each time step.

Such asynchronous models were studied experimentally in [FM05] and it was

shown that among the 256 elementary cellular automata (ECA), various qualitative responses to asynchronism were to be observed. Using both qualitative and quantitative observations, we proposed as a first step to divide the space of the ECA into four classes. The first class is composed of the "robust" ECA for which no major change occurs when the synchrony rate is varied. The second class is composed of the first-order phase transition-like ECA (PT1), for which an introduction of an infinitesimal quantity of asynchronism produces a major change in the behaviour. The third class is composed of the second-order phase transition-like ECA (PT2) which are robust to asynchronism up to a certain quantity and for which a brutal change of behaviour occurs when a given critical probability is attained. The fourth class is composed of the ECA for which the experimental protocol proposed did not produce regular curves.

In general, the repartition of each ECA in one of the four classes cannot be predicted easily ; in particular no obvious correlation with Wolfram's classification [Wol84] was noticed. In order to determine the convergence time of the asynchronous cellular automata, we analytically investigated the behaviour of the subclass of double-quiescent ECA for which both states are quiescent: the study of the convergence time to a fixed point allowed us to gain insight on how their global dynamical properties were linked to the local transition rule [FMST05].

The present work is devoted to understanding the class PT2 with an experimental approach. Improving the investigations first presented in [Fat06], we show that the singular behaviour of the rules found in this class can be explained by using models derived from statistical physics. The article is divided as follows: in the next section, we introduce directed percolation and draw a brief review of the observation of this phenomenon in the context of probabilistic CA. Section 2 presents the position of the problem in the scientific context. In Sec. 3, formal notations are introduced and in Sec. 4, some simple convergence properties are presented. Section 5 contains the protocol for measuring the dynamical exponents of the phase transition. Finally, we discuss the results in Sec. 6, putting them into the more general context of the study of the robustness of cellular automata.

2 Directed percolation in asynchronous or probabilistic CA

In this section, we present a short review of other works related to asynchronous or probabilistic cellular automata and directed percolation.

2.1 On asynchronism in CA

The problem of evaluating the change of behaviour of an asynchronous CA was at first addressed in [BI84] by means of simulation, the evaluation of the change in behaviour remaining qualitative. Other experimental works such

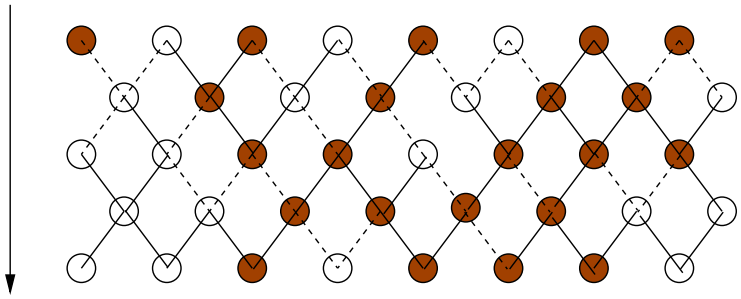

Figure 1: Illustration of an example of directed percolation: filled circles are wet sites, empty circles represent dry sites ; solid (resp. dashed) represent open (resp. closed) bounds.

as [BD94, SdR99, RZ02] followed, showing that the update scheme was indeed a key point to study. On the theoretical side, very few results have been obtained so far: the independence on the "update history" was shown undecidable in [Gác03], existence of stationary distributions was studied in [Lou02] and a first classification based on the convergence time was proposed in [FMST05, FMST06] and extended in [FRST06]. In the work [FM05], we proposed an experimental protocol to discriminate the ECA that alter significantly their behaviour when changing the synchrony rate from the those which remain robust.

This study showed that, among other phenomena, for seven elementary cellular automata, there exists a particular value of the synchrony rate α_c for which a small change of value produces an abrupt change of behaviour. It was then conjectured that this brutal variation could be explained by the existence of a phase transition, more precisely that the universality class of the phase transition was *directed percolation* (DP). We wish to emphasise that this hypothesis was mainly supported by the observation of the space-time diagrams produced near criticality.

2.2 Directed percolation

Percolation problems are well-known problems that have mainly been studied in both fields of discrete mathematics and statistical physics. They are motivated by the need to model situations in which a fluid has to evolve into a porous medium.

In the classical problem of *isotropic bond percolation*, the porous medium is discretised and modelled by a regular infinite square lattice. The nodes of the lattice, or *sites*, are linked by bonds which can also be in two states either *closed* or *open*. The links are distributed randomly, having a probability p to be open and a probability $1 - p$ to be closed. The sets of all sites connected through closed links is called a *cluster*. The problem of percolation is to determine the average size of a cluster as a function of p: it is easy to see that as this size

increases with p but what is most surprising is that in the two-dimensional case, the average cluster size diverges for the critical value $p_c = 1/2$. The physical interpretation of this result is that for $p > 1/2$, a fluid introduced in a given site may propagate at an arbitrary distance through the lattice.

Directed bond percolation can be seen as a non-isotropic variant of the previous model in which links are oriented according to a particular direction. It may model situations in which the fluid can go in only one direction as in the case of water submitted to gravity. Intuitively, as the propagation is more difficult to achieve, we have that the critical value p_c is higher than in the case of isotropic percolation.

We may also give an interpretation of directed percolation as a probabilistic dynamical system: sites have a state that is either *wet* or *dry*. Starting from one or several wet sites, the states of sites are updated according to the simple rule saying that a site becomes wet if it has one wet site linked to it through an open bound (see Fig. 1).

Theory and observations [Hin00a] predict that for an infinite regular lattice ($\mathbb{Z}^2$) and for a fixed value of p, if we start from an initial configuration with all sites in wet state, the density of wet sites $d(p,t)$ (*i.e.*, the limit ratio of wet sites in a given region over the size of the region) evolves to a positive limit for $p > p_c$ and to a zero limit for $p \leq p_c$.

More precisely, if we denote by $d_\infty(p)$ the infinite time limit of $d(p,t)$, the system obeys the following laws:

- for $p < p_c$, because the average size of clusters is finite, we have :
$$d_\infty(p) = 0$$
- for $p > p_c$, near the critical point, the asymptotic density diverges from zero by following a power law:
$$d_\infty(p) \sim (p - p_c)^\beta$$
- for the critical value $p = p_c$, the density vanishes to zero $d_\infty(p_c) = 0$ and the decrease follows a power law:
$$d(p_c, t) \sim t^{-\delta}$$

Note that as in all second order phase transitions, the function $d_\infty(p)$ is continuous but its derivative is not. Moreover, as we have $\beta < 1$, the right derivative of $d_\infty(p)$ has an infinite value at the critical point.

The exponents of the power-laws are called *critical exponents*, so far, their value $\delta = 0.1595$ and $\beta = 0.2765$ has been known by numerical simulations (the values are given here with four digits, see [Hin00a] for better precision). Many analytical methods have been proposed to approximate their value or to accelerate their calculus but it is so far an open problem to determine whether these exponents are rational numbers or not.

There are also other critical exponents that can be used to identify a universality class but we here choose to focus only on the measure of β and δ exponents (following [MZ98, Gra99] for instance).

2.3 The universality class of directed percolation

Many physical or numerical systems exhibit critical phenomena and it is remarkable that the laws governing the evolution of the system are generally power-laws near the critical point. Intuitively, one may understand the origin of these power-laws from the fact that near the critical transition point, the system has a self-similar fractal structure and thus no typical spatial wavelength. One surprising fact is that the same set of critical exponents may be found for different physical or numerical systems.

The collection of all phenomena that are described by a set of critical exponents is called a *universality class*. It is out of scope to list all the phenomena that where shown to belong to the directed percolation universality class and we refer to [Hin00a, Hin00b] for a review.

As far as cellular automata are concerned, directed percolation was observed in various problems. To our knowledge, the first CA that was shown to exhibit DP is the Domany-Kinzel cellular automaton [Kin83, DK84]. This model is a tunable probabilistic CA that have the ability to display two different transitions depending on the values of its parameters. Various other models involving some probabilistic CA tuned by an *ad hoc* control parameter were also shown to exhibit DP phenomena (*e.g.*, [ÓdorBS93, ÓdorS96]).

DP was also identified in problems involving synchronisation of two copies of cellular automata (*e.g.*, [Gra99, Rou06]). To our knowledge, the only example of directed percolation induced by asynchronism was given by Blok and Bergersen for the famous Game of Life [BB99]. The protocol they used to identify the universality class of the phase transition relied on the sole measure of the critical exponent β.

3 Formal definitions of the model

Let a ring of n cells be indexed by $\mathcal{L} = \mathbb{Z}/n\mathbb{Z}$, a *configuration* is an assignment of a state to each element of $\mathcal{L}$, the space of configurations is $E_n = \{0,1\}^{\mathcal{L}}$. An *elementary cellular automaton* (ECA) is described by a function $f : \{0,1\}^3 \to \{0,1\}$ called the *local rule*. Each ECA is indexed according to the usual notation [Wol84].

The probabilistic nature of the transitions leads us to introduce the notion of random configuration. Formally, a *random configuration* will be a probability distribution over the sigma-algebra composed by the set E_n and the sets of all subsets of E_n. Intuitively, a random configuration x can be understood as a function that assigns to each configuration $c \in E_n$ the probability to find x is in the state c if an observation is made.

Using the α-asynchronous updating scheme, the local rule f allows us to define a probabilistic global rule F which operates on the random variables

$(x^t)_{t\in\mathbb{N}}$ according to $x^{t+1} = F(x^t)$ such that:

$$\forall i \in \mathcal{L},\ x_i^{t+1} = \begin{cases} f(x_{i-1}^t, x_i^t, x_{i+1}^t) & \text{with probability } \alpha \\ x_i^t & \text{with probability } 1-\alpha \end{cases}$$

By taking $\alpha = 1$, we fall back on the classical synchronous case and as α is decreased, the update rule becomes more asynchronous while the effect of an update remains unchanged. The configuration x^t is a random variable that depends on the *sequence of updates*,*i.e.*, the sequence of subsets of $\mathcal{L}$ that are updated at each time step. For the sake of simplicity we do not explicitly formalise here the sequence of updates and the probability over the space of sequence of updates.

The *density* $d(c)$ of a configuration $c \in E_n$ is the ratio of cells in state 1 over the configuration size. In an abuse of notation, we denote by $\bar{d}(x^t)$ the average density, over all sequences of updates, of the random variable $d(x^t)$; it is our main parameter that we use to characterise the behaviour of a cellular automaton.

The synchrony rate α being fixed, for a given system size n, we denote by $d_\alpha(n,t)$ the average density at time t over all possible initial configurations of $x \in E_n$:

$$d_\alpha(n,t) = \frac{1}{2^n} \sum_{x\in E_n} \bar{d}(x^t)$$

Note that $d_\alpha(n,t)$ is also the the average density obtained started from a *uniform random configuration* of size n (*i.e.*, a configuration where each cell independently has a probability $1/2$ to be state `0` or `1`).

For some CA rules and some values of α, the sequence $(d_\alpha(n,t))_{n\in\mathbb{N}}$ may converge and we will call the limit, when it exists, the *asymptotic density at time t*, and denote it by $d(\alpha,t)$:

$$d(\alpha,t) = \lim_{n\to\infty} \frac{1}{2^n} \sum_{x\in E_n} \bar{d}(x^t)$$

Again, for some CA rules and some values of α, the sequence $(d(\alpha,t))_{t\in\mathbb{N}}$ may converge and we will call the limit, when it exists, the *asymptotic density*, and denote it by $d_\infty(\alpha)$:

$$d_\infty(\alpha) = \lim_{t\to\infty} d(\alpha,t) = \lim_{t\to\infty} \lim_{n\to\infty} \frac{1}{2^n} \sum_{x\in E_n} \bar{d}(x^t)$$

It is important to notice that the $\lim_{t\to\infty}$ and $\lim_{n\to\infty}$ operators, do *not* commute. In general, we have that:

$$d_\infty(\alpha) \neq \lim_{n\to\infty} \lim_{t\to\infty} \frac{1}{2^n} \sum_{x\in E_n} \bar{d}(x^t)$$

This non-commutativity has its importance when carrying the experiments. Indeed, because the system size and the sampling time are finite, it is important to determine in which order to correctly adjust the ring size n and the observation time t in order to get the best approximation of the asymptotic density. In particular, for the automata that are studied here, we claim that:

$$\lim_{n\to\infty}\lim_{t\to\infty}\frac{1}{2^n}\sum_{x\in E_n}\bar{d}(x^t)=0$$

This statement will not be proved here. Informally, we can note that as $0^{\mathcal{L}}$ is the only fixed point for rules 6, 18, 26, 50, 58, 106 ; and as there is always a sequence of updates of finite length (and thus of non-zero probability) that can bring the system to the fixed point $0^{\mathcal{L}}$; the system should eventually reach this fixed point. The case of ECA 146 is slightly different as it has two fixed points $0^{\mathcal{L}}$ and $1^{\mathcal{L}}$.

In other words all the *finite* size systems used for simulating DP are in a *metastable* state. By contrast, when we consider infinite-size systems, the transition phase hypothesis stipulates that there exists a non-empty interval such that $d_\infty(\alpha) > 0$ for all α in this interval.

4 First observations

The goal of this section is to give to the reader a first set of observations to understand the DP phenomenon in the case of asynchronous cellular automata.

4.1 Space-time diagrams

From [FM05], the rules that were experimentally detected as showing a brutal change of behaviour for a non-trivial value of α are ECA 6, 18, 26, 50, 58, 106, 146 and 178 (only "minimal representative rules" are considered).

Figure 2 shows how the variation of synchrony rate affects the space-time diagrams of three such rules. They were obtained starting from a *uniform random initial configuration*, *i.e.*, a configuration obtained by assigning to each cell an equal probability to be in the state 0 or 1 [1]. We see can divide the space-time diagrams into three categories:

- The synchronous behaviour which can of type "subshift" (ECA 6) or "chaotic" (ECA 18) or "periodic" (ECA 50).
- A behaviour with branching-annihilating patterns, observed on ECA 18 and 50 for $\alpha = 0.75$ and observed for ECA 6 for $\alpha = 0.25$. We call this behaviour the *supercritical phase*.

[1] Note that this definition only specifies a way of producing configurations and should not be considered as a mathematical definition of a certain type of configurations. (Given a configuration x there is no way of telling if x is a uniform random initial configuration.)

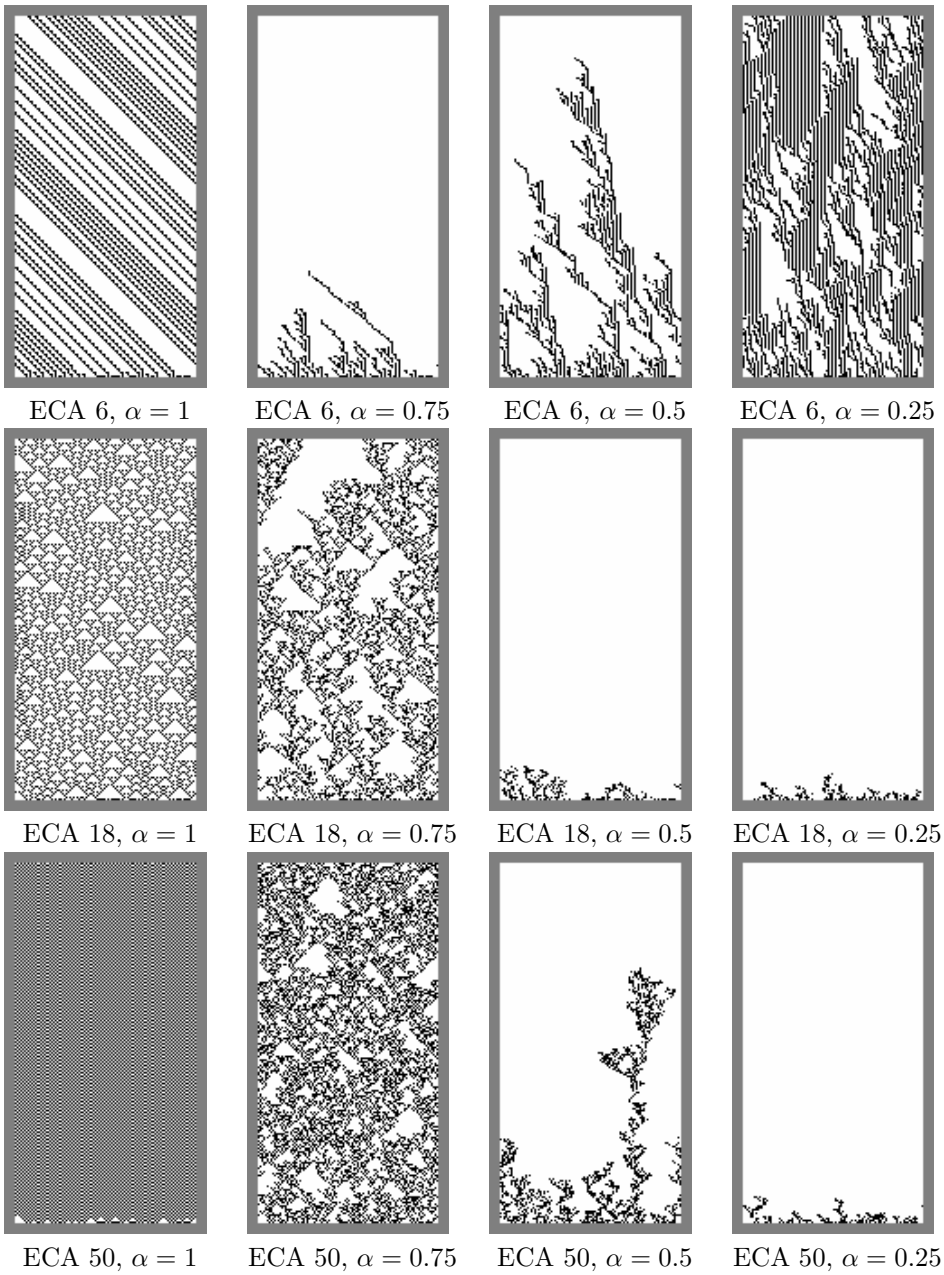

Figure 2: Space time diagrams for ECA 6 (top), ECA 18 (middle) and ECA 50 (bottom). Synchrony rate is decreased, from $\alpha = 1.00$ (leftmost) to $\alpha = 0.25$ (rightmost). Time goes from bottom to top; the time factor is rescaled by a factor $1/\alpha$ (i.e., for $\alpha = 0.25$ only time steps that are multiples of 4 are displayed).

- A behaviour of quick convergence to $0^{\mathcal{L}}$, observed for ECA 18 and 50 for $\alpha = 0.25$ and $\alpha = 0.50$ and for ECA 6 for $\alpha = 0.75$ and $\alpha = 0.5$. We call this behaviour the *subcritical phase*.

4.2 Approximation of the Asymptotic Density

The phase transition theory stipulates that there should be two macroscopic parameters, respectively called *the control parameter* and *the order parameter* such that the variations of the order parameter obey to the DP power laws when the control parameter is varied. For sake of simplicity, we propose here to use the synchrony rate α as a control parameter and the density d as an order parameter. However, note that other possibilities may also be examined, for example in [BB99] the authors also use the *activity* (*i.e.*, the ratio of cells in an unstable state) as an order parameter.

In order to quickly test this hypothesis, we varied α with small increments (1%) and, starting from a uniform random initial configuration of size $n = 10^4$, we measured the average density during 10^3 steps after waiting 10^4 steps to let the system stabilise. Figure 3 shows how this rough approximation of the asymptotic density varies with α.

We observe that the first seven plots show a good regularity, and have a behaviour that is compatible with a second order phase transition and thus with DP : the density vs. alpha plot is a continuous curve that reaches zero with an infinite slope (the derivative of the function is not continuous). ECA 178 exhibits a different behaviour is excluded from our set of DP candidates. Note that as ECA 6 has an "inversed" phase-transition, the respective place of the sub- and super-critical phases is inverted.

This means that for these seven identified *DP-ECA*, we expect to measure :

$$d(\alpha_c, t) \sim t^{-\delta}$$

and

$$d_\infty(\alpha) \sim {\Delta_\alpha}^{\beta} \text{ for the supercritical phase}$$

with $\Delta_\alpha = \alpha_c - \alpha$ for ECA 6 and $\Delta_\alpha = \alpha - \alpha_c$ for the six other DP-ECA. Naturally, these power laws can be obtained only for infinite-size systems. As simulation requires finite lattices, we are bound to introduce finite-size effects. This means that all the measures will be subject to noise and to systematic errors. The main difficulty in DP measurements consists in minimising both type of errors by a carefully designed Monte Carlo simulation protocol.

4.3 A close-up for the initial times

In the sequel, we will systematically present the curves for ECA 50 while the numerical data will be given for the seven DP-ECA. Indeed, this rule can be written in the rather simple form:

$$\forall (a,b,c) \in \{0,1\}^3,\ f(a,b,c) = \begin{cases} 1-b & \text{if } (a,b,c) \neq (0,0,0) \\ 0 & \text{if } (a,b,c) = (0,0,0) \end{cases}$$

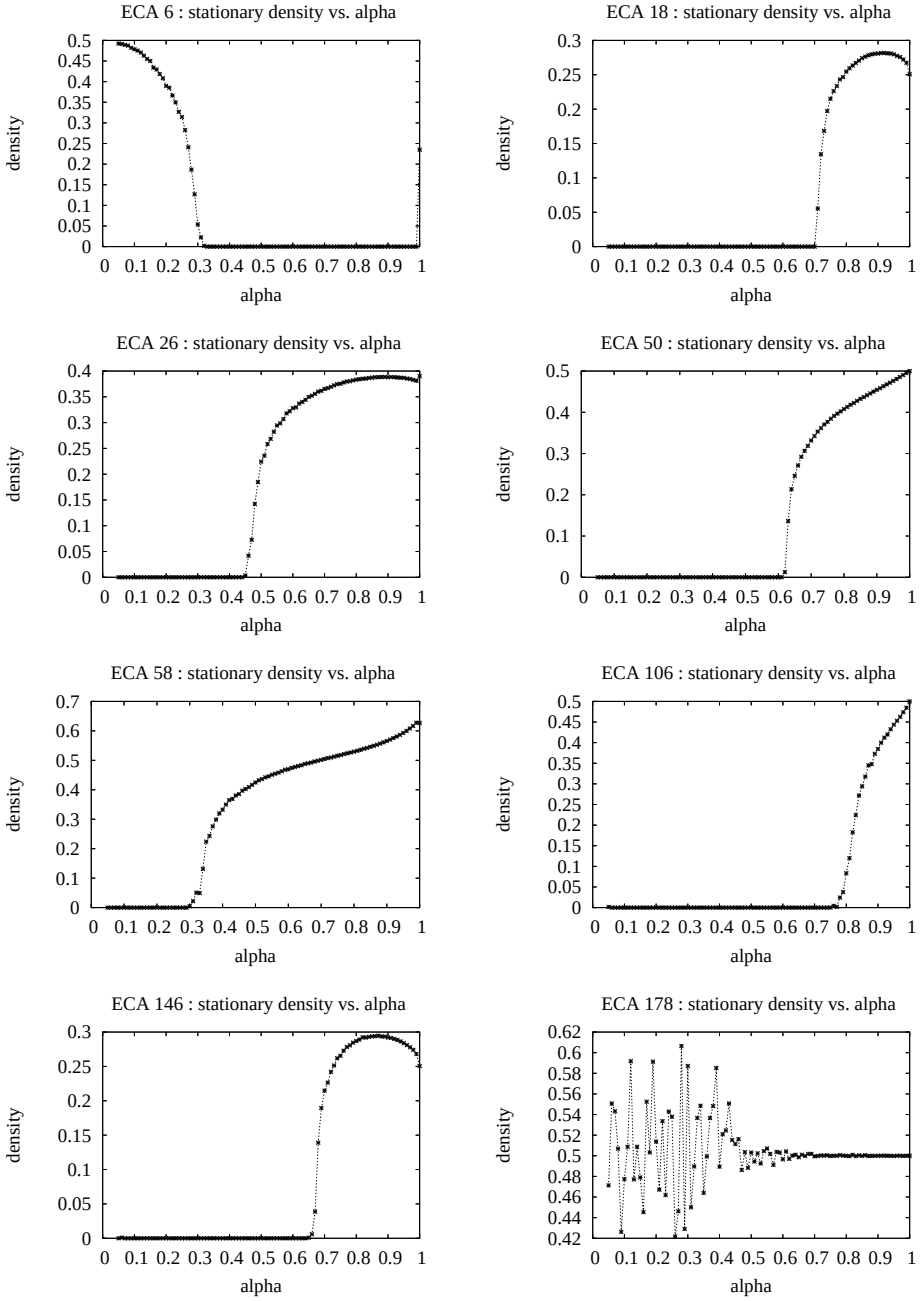

Figure 3: Asymptotic density as a function of the synchrony rate ; it is estimated by the computation of the average density obtained on a sampling time $S = 10^3$, after a transient time $T = 10^4$ has elapsed. Note the change of scale in the y-axis.

It is possible to see this rule as a one dimensional version of an "epidemic" rule: a healthy cell (state 0) gets infected (state 1) if at least one of its neighbour is infected ; once it is infected, it becomes healthy at the next updating.

For ECA 50, the previous experiment allows us to locate the critical synchrony rate around $\alpha_c \sim 0.62$. However, it should be made clear if the shape of the plot obtained varies when the initial configuration is changed, or when the sequence of updates is changed, or when the system size, the transient and sampling time are increased. Do we observe the same type of abrupt transition? Does this transition still occur at the same point?

In order to clarify these questions we briefly examined how the system size, the sequence of updates and the initial configuration would influence the evolution of the density for a short range of time (the first hundred steps). Figure 4 shows the evolution of the density for ECA 50 evolved with synchrony rate $\alpha = 0.62$, fixed or different initial configurations, with fixed or different sequence of updates and ring size $n = 2\ 10^3$ and $n = 2\ 10^4$.

The first plot (4.A) shows the temporal evolution of the density with different sequences of updates, applied to three different random initial configurations of densities 0.10, 0.20, and 0.50. We see that the system quickly converges to a "mean-behaviour" that seems independent of the initial configuration. So this "initial configuration forgetting" property is strongly reminiscent of a "Markovian" property: the plots have a tendency to merge in a few hundred steps. However, note that because of the property of metastability (see Sec. 3 page 7) this is not strictly a Markovian property as the only reachable fixed distribution is the zero density.

One may also examine if it is necessary to generate different sequences of updates to obtain these plots. Indeed, as the random number generation is a time-consuming operation, one could speed up the process by using the same numbers for generating the Monte Carlo sequence of updating.

The second plot (4.B) shows that applying the same sequence of updates to different initial configuration does not modify the results substantially. However, a close examination of the curves shows that small correlations appear from time to time. These correlations are visible by noting that there exists repetitive tendencies to oscillate in the same directions around a mean behaviour ; they indicate that the system is sensitive to the updating sequence. It is not as sensitive as ECA 46 for example (see [FM05, Rou06]) but this means that it is *not possible* to use the same sequence of updates with different initial configurations to obtain the average behaviour.

Finally, a quick visual examination of what happens when we start from the same initial configuration and use different updates did not allow us to detect any similar "correlation". In Fig. 4.C, the plots shows that the curves oscillate around a mean-value. Of course more analysis is needed to ensure that no hidden correlation are present but these observations are coherent with directed percolation predictions.

In all this experiments, the increase of ring size n did not produce any significant change apart from having smoother curves. Indeed, increasing the system size is somehow equivalent to doing an averaging.

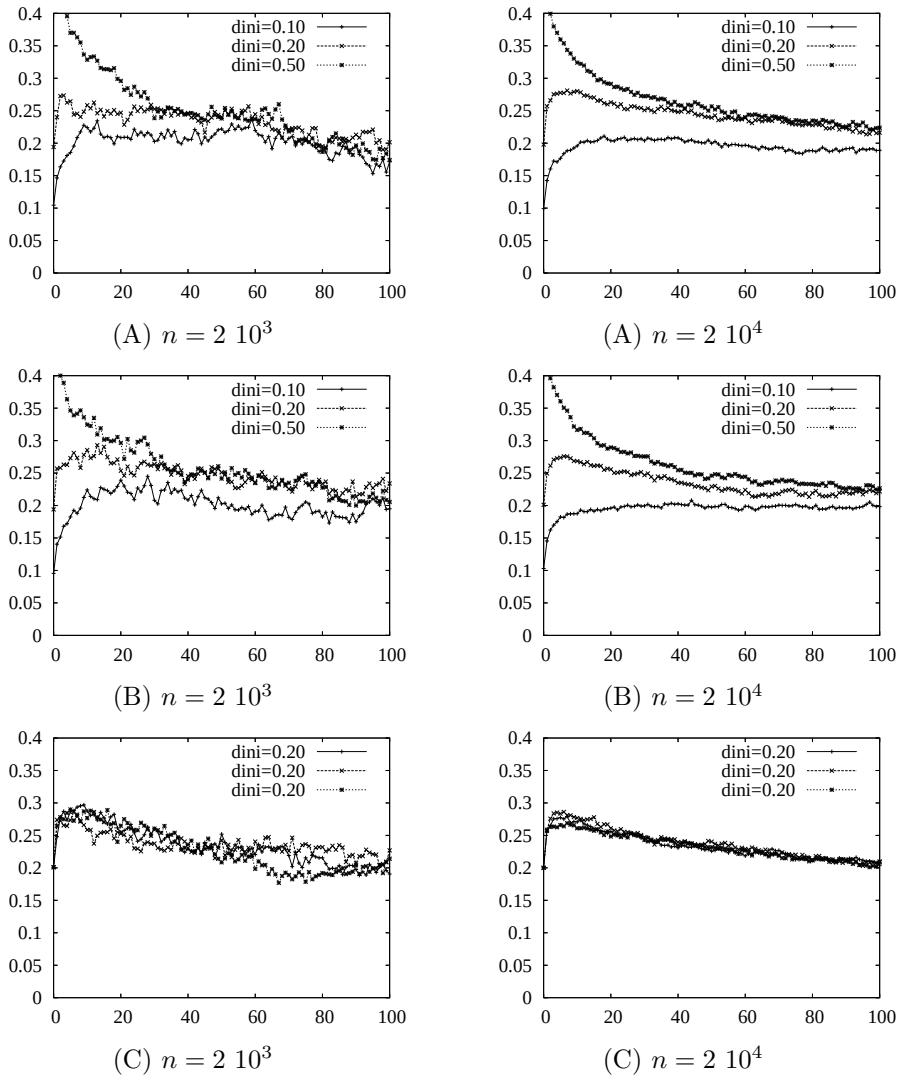

Figure 4: ECA 50: Evolution of the density for different system settings. The ring size is varied with $n = 2\ 10^3$ (left) and $n = 2\ 10^4$ (right). (A) Different sequence of updates and different initial densities. (B) Fixed sequence of update and different initial density. (C) Different sequence of updates and same initial configuration.

This small set of experiments suggests that it should be possible to measure the asymptotic density $d_\infty(t)$ by making an average on the Monte Carlo simulations. All the runs will start from the same initial configuration, a uniform random configuration of size n and the sequence of update will be varied, using the `Ranmar` random number generator (period $\sim 10^{43}$) implemented on the `FiatLux` cellular automata simulator [Fat]. Note that this is coherent with other DP experiments in which the initial configuration is fixed, often chosen as a homogeneous configuration in which all the cells or nodes are in the same state. Here, the configuration $\mathtt{1}^{\mathcal{L}}$ could also be used but it would create a problem for ECA 146 as it is a fixed point for this automaton.

5 Protocol

The measure of DP-critical exponents is a delicate operation that generally requires large amount of computation time. The main difficulty resides in avoiding systematic errors when obtaining statistical data near the transition point. For example, it happened that authors were mislead by their measures and concluded that a phase transition phenomenon was not in the DP universality class [MZ98], which was later proved wrong [Gra99] by using a different protocol and more precise measures.

In order to limit the influence of systematic errors, we use the two-step protocol that was used by Grassberger in [Gra99]:

- We measure the critical synchrony rate α_c by varying α until we reach the best approximation of a power-law decay for the density. This first experiment also allows to measure the critical exponent δ.
- We measure the asymptotic density d_∞ as a function of α and then fit a power-law in order to calculate β.

Note that these two steps are not independent since the second operation uses the previously computed value of α_c.

5.1 First critical exponent: δ

Preliminary observation

Figure 5 shows the temporal decay of the density for ECA 50 as α is varied by 10^{-3} increments from 0.626 to 0.630. The curves are obtained by averaging the data on $N_s = 100$ runs of time $T = 2.10^5$. We see that as α is increased, the curve in a log-log plot transforms from a concave function to a convex function. Visually, we see that this transformation is obtained for $\alpha = 0.628$. As predicted, we see that the curve's slope in its linear part is close to $-\delta_{\mathrm{DP}} = -0.1595$.

Table 1: Variation of the critical synchrony rate as a function of the scaling factor (ECA 50).

n ($\times 10^4$)	1/4	1/2	1	2	4	8
α_c	0.6287	0.6283	0.6282	0.6281	0.6282	0.6282

Calibrating the experiment

If we want to increase the precision of the critical synchrony rate, we need to repeat the experiments with a smaller increment of α. However, the limitations of computing time require to tune carefully the different parameters of the protocol. If we fix the increment of α to 10^{-4}, the trade-off concerns the lattice size n, the number of runs for a measure N_s and the time of observation T.

In [Fat06], we experimentally observed that taking $N_s = 100$ with lattice size $n = 10^4$ was a good setting to reduce the noise of the curves for times smaller than $T = 10^6$. Figure 9 shows $\sigma(t)$ the standard deviation of the sequence of the $N_s = 100$ measures of $d(t)$ for $t \in [10^2, 10^6]$ and $n = 2\ 10^4$. It is interesting to note that this standard deviation seems to increase as a power law. If we approximate the noise amplitude at time t by the quantity $\sigma(t)/\sqrt{N_s}$, we see that this noise amplitude keeps a small value (less than $2\ 10^{-3}$ for $t = 10^6$). This is why we need to plot it in a separate figure, as the width of error bars wouldn't be large enough if plotted on the $d(t)$ curves of Fig. 5.

Scaling of the phenomenon

Then, in order to examine to which extent the measure of critical synchrony rate α_c depends on the lattice size n, we conducted a experiments with fixed $N_s = 100$ and $T = 10^6$ and varying the lattice size from $n = 2.5\ 10^3$ to $n = 8\ 10^4$. For ECA 50, Table 1 shows that α_c decreases as n increases and that the value observed converges to 0.6282 ± 10^{-4}. For a lattice size greater or equal than $n = 10^4$, the value of α_c seem to converge with a precision smaller than the increment of α (10^{-4}). This observation allows us to fix the value of n to 2.10^4 as a further increase in the lattice size would not necessarily result in obtaining a precision smaller to 10^{-4} in the determination of α_c. In other words, this means that the precision gained by studying the scaling of the phenomenon becomes smaller than the noise. Note that this experiment is time-consuming as the computation requires more than 10^{14} applications of the local rule.

Measurement of α_c

Keeping the settings $n = 2\ 10^4$ and $N_s = 100$, we measured the evolution of the density for the seven DP-ECA during a sampling time up to $T = 10^7$, depending on the automata considered. Note that because we expect a linear curve in a log-log plot, we sampled the density with an exponential interval. This allows us to speed up the computation and provides a way of shrinking the arrays of data to approximately a hundred samples.

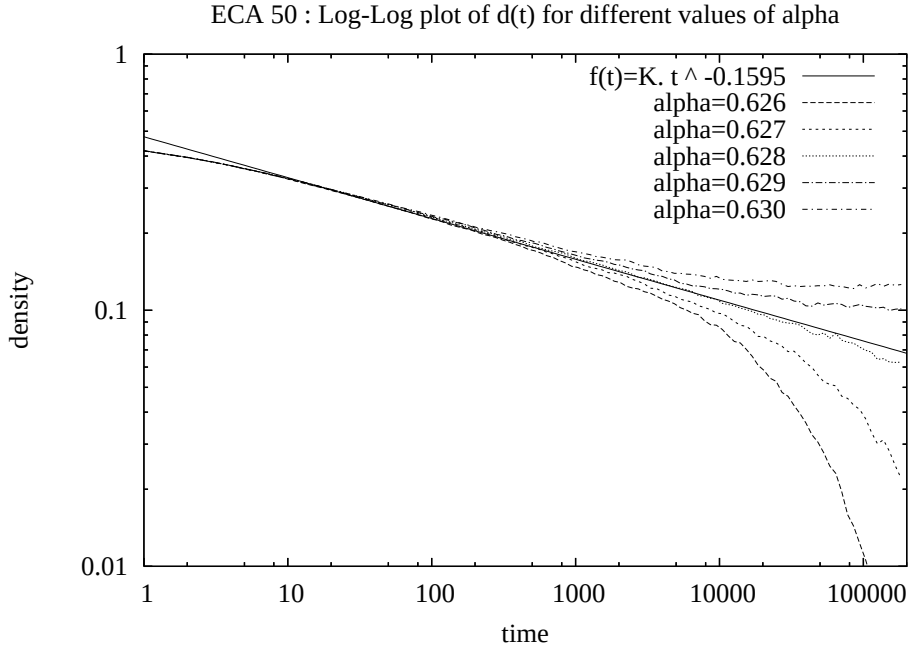

Figure 5: ECA 50: Determination of the critical synchrony rate α_c. Averages obtained on $N_s = 100$ runs and ring size $n = 2\ 10^4$. These conditions are kept in the following. The straight line has slope $-\delta_{DP} = -0.1595$ and is plotted for reference. α is varied by increments of 10^{-3}, for $2\ 10^5$ simulation steps.

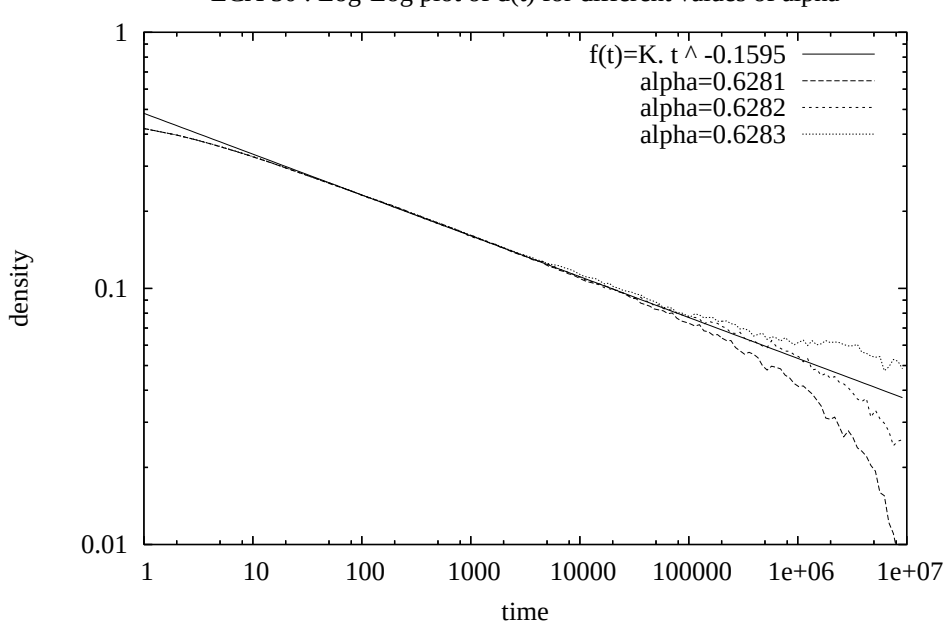

Figure 6: α is varied by increments of 10^{-4}, for 10^7 simulation steps.

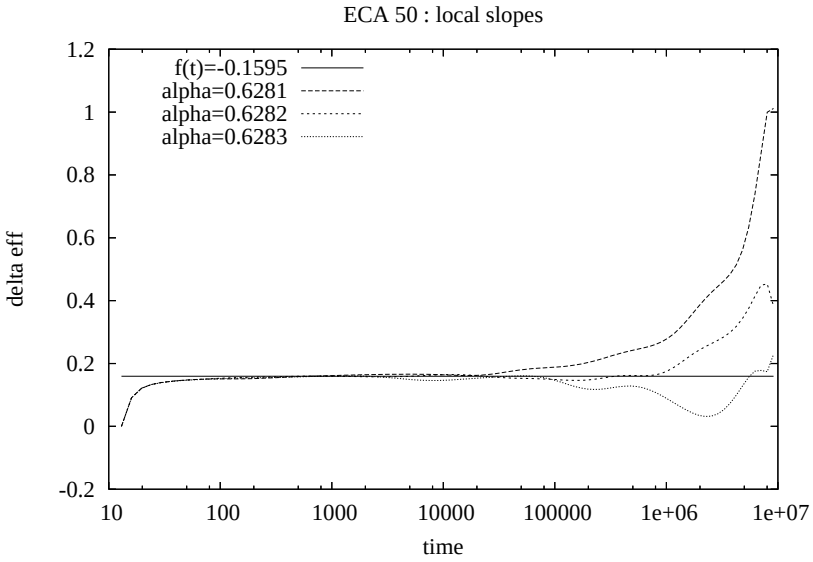

Figure 7: ECA 50: Determination of local slopes with m=10. The curves are plotted after the application of a smoothing procedure (Bézier type).

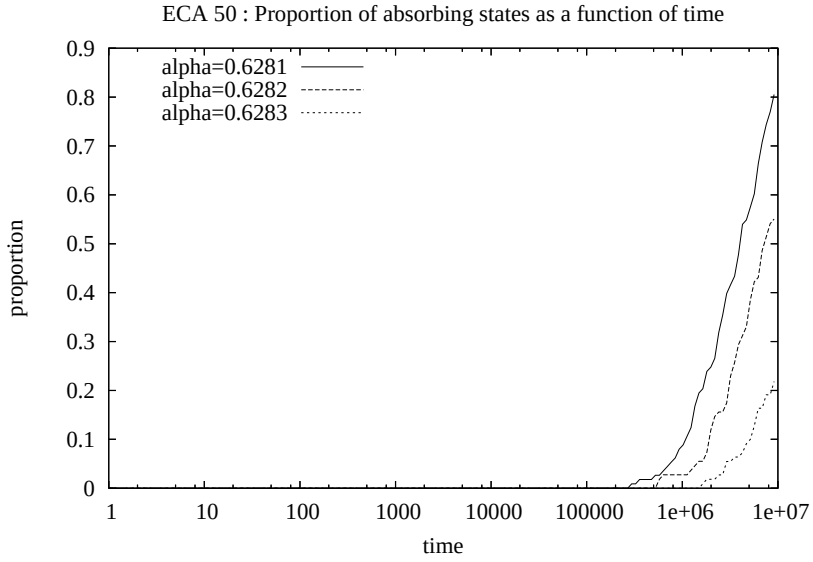

Figure 8: ECA 50: Proportion of absorbing states as a function of time.

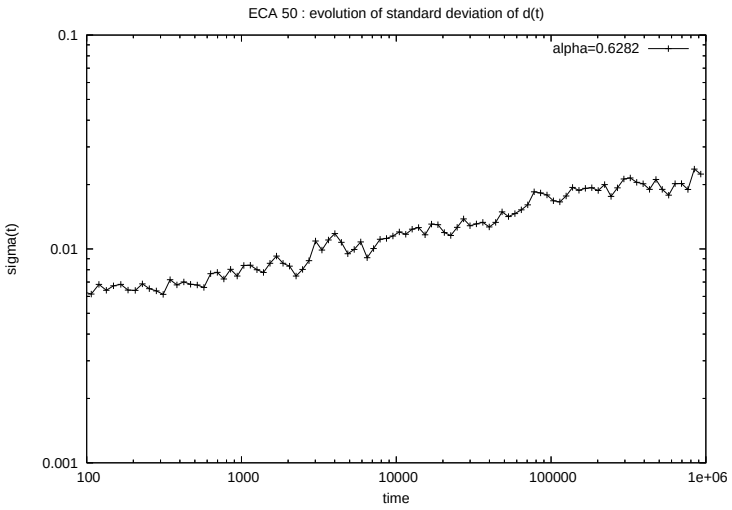

Figure 9: ECA 50: Logarithmic plot of the evolution of the standard deviation of the random variable $d(t)$.

The result for ECA 50 is plotted in Fig. 6. It clearly allows us to discriminate between the convex-shaped curve obtained for $\alpha = 0.6281$ and the concave-shaped curve obtained for $\alpha = 0.6283$ [2].

For each set of measures, the convexity of the curves was determined both visually and numerically. A visual tool to discriminate the plots consists in plotting the local slope (see [Hin00a]) as a function of time according to:

$$\delta_{\mathrm{loc}}(t) = \frac{\log d(t) - \log d(t/m)}{\log t - \log(t/m)} = \frac{\log\left[d(t)/d(t/m)\right]}{\log m}$$

with m varying between 4 and 10 (heuristic criterion).

Figure 7 shows the evolution of the local slope with time. One may distinguish three parts in the evolution of the system: a "transient" part, a "power-law" part and the departure from power law. If the length of transient part only depends on the ECA considered, the length of the "power-law" part of the curve is a function of the discrepancy between the value of its synchrony rate α and the critical synchrony rate α_{c}: the smaller this value, the longer the system will follow the power-law predictions. One may also notice that the three curves tend to have an increase of their local slope for simulation times greater than $2\ 10^6$. If we recall that the system is in a metastable state (see Sec. 3), this surprising effect can be easily understood by looking at the each time step, the proportion of runs which have reached the fixed point $0^{\mathcal{L}}$. The temporal evolution of this proportion is shown in Fig. 7 ; from this plot we can deduce that for our choice of system size $n = 2\ 10^4$, the convexity of the curves has to be examined for simulation times greater than $2\ 10^6$.

[2] The set of the other curves is provided in Annex : see Fig. 12 page 25.

The two values of synchrony rate $\alpha_{\min}$ and $\alpha_{\max}$ for which the change of convexity was observed are reported in Table 2 page 21.

Measurement of δ

In order to obtain an estimation of δ, we computed the slopes of the linear part of the curves for $\alpha_{\min}$ and $\alpha_{\max}$. The corresponding values of the slopes, $\delta_{\min}$ and $\delta_{\max}$ are given in Table 2 for comparison with δ_{DP}. We took $t \in [2\ 10^3, 2\ 10^5]$ as a fit interval to compute this slope. The lower limit is obtained by a rough estimation of the transient time needed for the system to enter into the power-law regime. The upper limit of the interval corresponds to the moment when deviation from a power-law decay becomes visually observable for two curves obtained with a variation of α of 10^{-4}.

We wish to call the reader's attention on the fact that it is a difficult problem to estimate the error on δ. Indeed, besides the problem of estimating the influence of noise on the computed slopes, there is the problem of choosing properly the time interval in which to perform this fit. This motivates the presentation of the estimation δ as an interval rather than a value associated to a precision measure. Note that the bounds of the intervals are themselves subject to an imprecision of the order of 10^{-3}.

Given these estimations of uncertainty, we see that the observed intervals show good agreement with $\delta_{\mathrm{DP}} = 0.1595$.

5.2 Determination of β

The second part of the experiments consists in measuring the critical exponent β using the values of the asymptotic density as a function of α. Recall that, as α approaches α_{c}, the asymptotic density vanishes as: $d_\infty(\alpha) \sim {\Delta_\alpha}^\beta$.

Calibration of the experiment

To estimate this asymptotic density, it is necessary to adjust the sampling time as a function of Δ_α. Indeed, as Δ_α approaches zero, d_∞ approaches zero and the time needed to reach this density increases exponentially with $1/\Delta_\alpha$. This phenomenon, known as *critical slowing down* (*e.g.*, [Hin00a]), limits the precision on the measure of the asymptotic density d_∞.

In this experiment, we need to choose an interval of variation of Δ_α, for each value of Δ_α, we have to repeat N_{s} times the measure of $d(t)$ during a time T and then extrapolate the asymptotic density from this sampling. There are two different possibilities for varying Δ_α, some authors use linear variation (*e.g.*, [BB99]) while others use an exponential variation. As we expect the curve d_∞ vs. Δ_α to be linear in a log-log plot, we prefer to choose the exponential increment in order to have a equally spaced points in this plot.

The quantity $\Delta_\alpha = \alpha - \alpha_{\mathrm{c}}$ was varied according to an exponential increment of $\sqrt{2}$ from $2\ 10^{-4}$ to $2\ 10^{-1}$ (three orders of magnitude). For each point, we took $N_{\mathrm{s}} = 10$ and sampling times were fixed to $T = 10^6$ for all the values of Δ_α. Figure 10 shows the evolution of the density as a function of time for different values of synchrony rate.

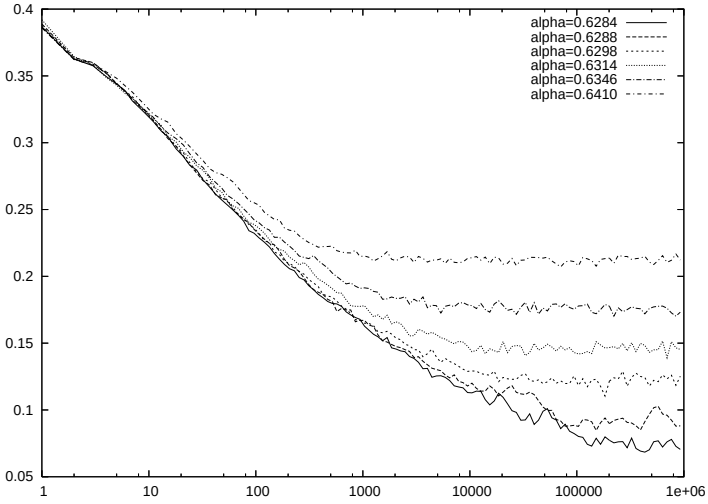

Figure 10: ECA 50: Evolution of the density vs. time for $\alpha > \alpha_c$, ring size $n = 2\ 10^4$, averaged on $N_s = 10$ runs, with sampling time $T = 10^6$.

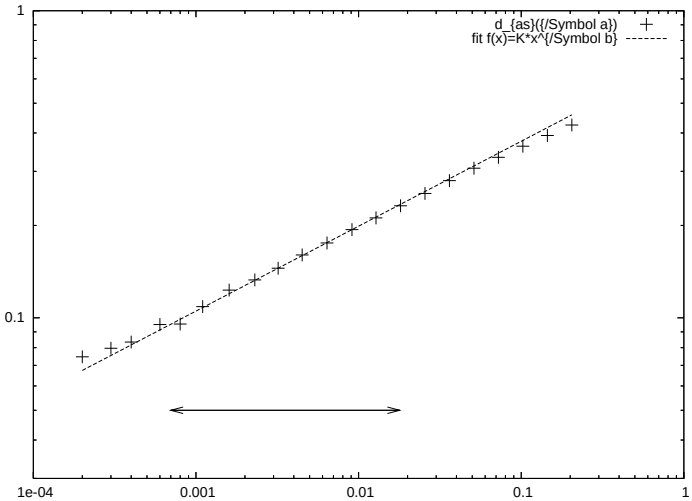

Figure 11: ECA 50: Determination of the critical exponent β using the time decay properties (see text). The straight line shows theoretical prediction and has slope: $\beta_{DP} = 0.2765$. Note that both x and y axis are displayed in logarithmic scale. The arrow shows the fit interval used to calculate the β exponents.

Table 2: Intervals for critical synchrony rate α_c and critical exponents δ and β.

Tr code	ACE	$[\alpha_{\min}, \alpha_{\max}]$	$[\delta_{\min}, \delta_{\max}]$	$[\beta_{\min}, \beta_{\max}]$
BFGH	6	[.2824, .2826]	[.158, .163]	[.263, .284]
BCEFGH	18	[.7138, .7140]	[.144, .164]	[.256, .279]
BCEGH	26	[.4748, .4750]	[.155, .167]	[.266, .283]
BCDEFGH	50	[.6281, .6283]	[.147, .168]	[.264, .281]
BCDEGH	58	[.3397, .3400]	[.156, .171]	[.270, .284]
BDEH	106	[.8145, .8147]	[.157, .161]	[.257, .278]
BCEFG	146	[.6750, .6752]	[.152, .162]	[.270, .287]

The asymptotic density $d_\infty(\alpha)$ was approximated by taking the average of the densities computed in the time interval from 5 10^5 to 10^6. Ideally, it would have been more efficient to adjust the sampling time as a function of Δ_α but at the time, we do not know how to make this adjustment.

Measurement of β

Figure 11 shows the approximated values of d_∞ as a function of Δ_α. The visual comparison to the expected slope β_{DP} shows good agreement.

Again, we notice that the linear part of the curves is limited by two competing phenomena. On the one hand, the small values of Δ_α are overestimated because of the critical slowing down (waiting longer means decreasing the value). On the other hand, for the higher values of Δ_α, the system "saturates" and no longer follows a power-law. The deviation from the power law is a phenomenon that is predicted by theory and that can be studied for its own interest. However, we prefer here to restrict our measures to the linear part of the curve.

By taking $\Delta_\alpha \in [8\ 10^{-4}, 128\ 10^{-4}]$ as a fit interval (see Fig. 11), by taking for α_c the three values 0.6281 , 0.6282, 0.6283, we respectively obtained for β: 0.281 , 0.274 , 0.264, leading to the uncertainty interval $[0.264, 0.281]$. Note that again the bounds of the interval are themselves subject to an imprecision of the order of 10^{-3}.

The same experiment was conducted for the seven ECA and the calculated values are shown in Table 2. Again, the computed values of β are in good agreement with the reference value $\beta_{\mathrm{DP}} = 0.2765$.

6 Discussion

The problem of determining how changes of behaviour were triggered by gradual changes in the update rule were investigated by numerical simulations. The results show good evidence that the phenomenon observed for seven asynchronous elementary cellular automata is a second order phase transition which belongs to the directed percolation universality class.

6.1 Grassberger's conjecture

The observation of the synchronous behaviour of the seven ECA studied indicate that there is certainly no straightforward relation with the existing classifications. For example, ECA 6, 50 and 58 are "periodic" (or Wolfram class II) rules while ECA 18, 26, 106 and 146 are "chaotic" (or Wolfram class III) rules. This indicates that near a critical point, asynchronous updating may render the details irrelevant at the microscopic cell-scale while the system is still governed globally by the same global laws. This further indicates that the observation of the synchronous behaviour of a CA does not fully catch the complexity of a rule since asynchronous updating may unveil another type of complexity.

These results may also be discussed in the light of a famous conjecture by Janssen and Grassberger (see [Hin00a] for a short presentation) that states that a model should belong to the DP universality class if it satisfies the following criteria:

a) the model displays a continuous phase transition from a fluctuating active phase into a unique absorbing state,

b) the possibility to characterise the phase transition by a positive one-component order parameter,

c) the definition of dynamics by short-range process,

d) and the absence of additional symmetries or quenched randomness (*i.e.*, fixed topological modifications).

For the seven DP-ECA, condition a) is fulfilled with $\mathtt{0}^{\mathcal{L}}$ as the absorbing state. For the six first DP-ECA, $\mathtt{0}^{\mathcal{L}}$ is the only fixed point but it is remarkable that for ECA 146, $\mathtt{1}^{\mathcal{L}}$ is also a fixed point. This shows that the informal notion of "absorbing state" can not be identified with the fixed point mathematical property.

Condition b) was fulfilled by the density parameter, in some other studies (*e.g.*, citeBlo99) it was also shown that counting the ratio of unstable cells was also a possibility for having another "order parameter".

Condition c) is true by definition of CA.

Condition d) is interesting as it clearly makes a difference between space symmetry, which is possessed by rules 18, 50, 146, and state symmetry (*i.e.*, invariance under `0` and `1` exchanging), which is absent for all the DP rules. It may also explain why rule 178, which has both symmetries, was also detected as having a phase transition but was not found into the DP universality class.

These four conditions are thus necessary but are not sufficient. It is indeed possible to find many ECA rules (*e.g.*, rule 74) that fulfil them but for which there exists no phase transition. So, one of the most challenging question now consists in explaining why only one small part of the CA that fulfil the four conditions above exhibit DP behaviour.

Table 3: List of the eight active transitions used in the labelling of ECA.

A	B	C	D	E	F	G	H
000 1	001 1	100 1	101 1	010 0	011 0	110 0	111 0

Table 4: Illustration of the branching phenomenon with three examples of labelled configurations. Bold labels show the cells were the transition occurs

label		b	f	**g**	**c**	
t	0	0	1	1	0	0
t+1	0	0	1	0	1	0

label		**b**	**e**	**c**	
t	0	0	1	0	0
t+1	0	1	0	1	0

label		b	f	**h**	g	c	
t	0	0	1	1	1	0	0
t+1	0	0	1	0	1	0	0

6.2 Examining the notation by transitions

It is difficult to find a common property for the seven DP-ECA by the simple examination of their transition table. In [Fat04, FMST05], we introduced the notation by transitions, which associates to each ECA the list of its active transitions (*i.e.*, transitions that change the state when applied) according to the labelling displayed in Tab. 3. It is interesting to notice that the seven DP-rules have the codes: BFGH, BCEFGH, BCEGH, BCDEFGH, BCDEGH, BDEH, BCEFG. We see that the E transition is present in all rules but rule BFGH, which is ECA 6 and which has a special behaviour. Moreover, there is a minimal number of four active transitions in each rule. We can gain some insight if we think DP as a competing process between branching and annihilation. So the E rule represents the possibility for annihilation by erasing a single `1` surrounded by two `0`. The branching can occur in different ways the most simple cases are illustrated in Tab.4.

6.3 Perspectives

At this point, a more detailed study on the interaction between transitions is needed. Such a study would probably open a possibility of investigations on how a reduction between different rules could be done. Another question to examine would be to see how dynamics of asynchronous ECA can be mapped with other well-studied phenomena such as synchronisation of configurations [Gra99] or Domany-Kinzel probabilistic CA [DK84]. However, such a reduction does not appear simple since ECA 6 has an "inversed" phase transition: the subcritical (frozen) state is reached by the *increase* of the synchrony rate. Another possibility for uniting the study of all the DP-ECA is to consider a particular rule with a particular synchrony rate as a point in the bigger space of probabilistic elementary cellular automata. In this space, which is homeomorphic to $\mathbb{R}^8$, it would be interesting to determine the frontiers where such phase transitions occur, in particular to know whether the DP-phase transition can be explained

in terms of crossing of a hypersurface.

From the point of view of possible applications, the most difficult challenge is to find examples of such phase transitions in nature or to use them in artificial systems. For example, it has been conjectured that mechanism could help explaining the trigger of the self-organisation phase in cellular societies [Fat03, Ber03]. In an engineering context, the fact that a distributed system may change its behaviour in a totally decentralised way is interesting to study. In the case were brutal changes of dynamics are desired, exploiting phase transitions could allow a system to change its behaviour without any centralisation of information, for example for performing a self-diagnosis.

7 Annex

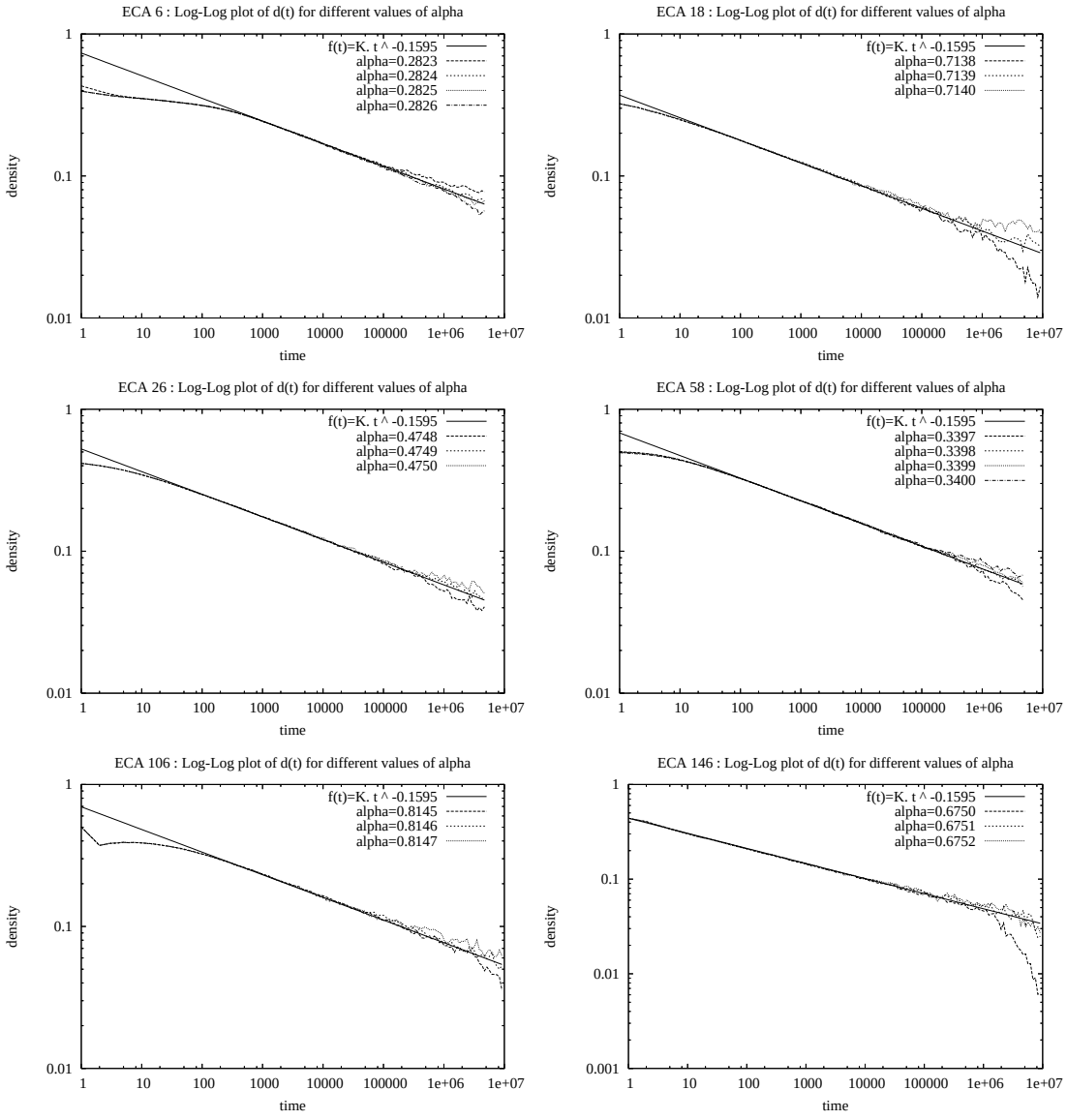

Figure 12: Evolution of density as function of time for the DP-ECA (except rule 50). All but ECA 18 are calculated with $n = 2\ 10^4$ and $N_s = 100$. ECA 18 is calculated with $n = 4\ 10^4$ for better discrimination of phases. ECA 6, 26, 58 are sampled with $T = 10^7$; ECA 18,106, 146 are sampled with $T = 5\ 10^6$.

References

[BB99] Hendrik J. Blok and Birger Bergersen. Synchronous versus asynchronous updating in the "game of life". *Physical Review E*, 59:3876–9, 1999.

[BCG82] Elwyn R. Berlekamp, John H. Conway, and Richard K. Guy. *Winning Ways for your Mathematical Plays*, volume 2. Academic Press, ISBN 0-12-091152-3, 1982. chapter 25.

[BD94] Hugues Bersini and Vincent Detours. Asynchrony induces stability in cellular automata based models. In Brooks, R. A, Maes, and Pattie, editors, *Proceedings of the 4th International Workshop on the Synthesis and Simulation of Living Systems $ArtificialLifeIV$*, pages 382–387. MIT Press, July 1994.

[Ber03] Hugues Berry. Nonequilibrium phase transition in a self-activated biological network. *Physical Review E*, 67:031907, 2003.

[BI84] Buvel, R.L. and Ingerson, T.E. Structure in asynchronous cellular automata. *Physica D*, 1:59–68, 1984.

[DK84] Eytan Domany and Wolfgang Kinzel. Equivalence of cellular automata to ising models and directed percolation. *Physical Review Letters*, 53:311–314, 1984.

[Fat] Nazim Fatès. Fiatlux CA simulator in Java. Available from `http://nazim.fates.free.fr`.

[Fat03] Nazim Fatès. Experimental study of elementary cellular automata dynamics using the density parameter. In *Discrete models for complex systems, DMCS '03 (Lyon)*, Discrete Mathematics Theoretical Computer Science Proceedings, AB, pages 155–165. Assoc. Discrete Math. Theor. Comput. Sci., Nancy, 2003.

[Fat04] Nazim Fatès. *Robustesse de la dynamique des systèmes discrets : le cas de l'asynchronisme dans les automates cellulaires.* PhD thesis, 'Ecole normale supérieure de Lyon, 2004.

[Fat06] Nazim Fatès. Directed percolation phenomena in asynchronous elementary cellular automata. In Samira El Yacoubi, Bastien Chopard, and Stephania Bandini, editors, *7th International Conference on Cellular Automata for Research and Industry Proceedings*, volume 4173 of *LNCS*, pages 667–675. Springer, 2006.

[FM05] Nazim Fatès and Michel Morvan. An experimental study of robustness to asynchronism for elementary cellular automata. *Complex Systems*, 16:1–27, 2005.

[FMST05] Nazim Fatès, Michel Morvan, Nicolas Schabanel, and Eric Thierry. Fully asynchronous behavior of double-quiescent elementary cellular automata. In Joanna Jedrzejowicz and Andrzej Szepietowski, editors, *Mathematical Foundations of Computer Science Proceedings*, volume 3618 of *Lecture Notes in Computer Science*, pages 316–327. Springer, 2005.

[FMST06] Nazim Fatès, Michel Morvan, Nicolas Schabanel, and Eric Thierry. Fully asynchronous behavior of double-quiescent elementary cellular automata. *Theoretical Computer Science*, 362:1–16, 2006.

[FRST06] Nazim Fatès, Damien Regnault, Nicolas Schabanel, and Eric Thierry. Asynchronous behavior of double-quiescent elementary cellular automata. In José R. Correa, Alejandro Hevia, and Marcos A. Kiwi, editors, *LATIN 2006 Proceedings*, volume 3887 of *Lecture Notes in Computer Science*, pages 455–466. Springer, 2006.

[Gác03] Peter Gács. Deterministic computations whose history is independent of the order of asynchronous updating. `http://arXiv.org/abs/cs/0101026`, 2003.

[Gra99] Peter Grassberger. Synchronization of coupled systems with spatiotemporal chaos. *Physical Review E*, 59(3):R2520, March 1999.

[HG93] Bernardo A. Huberman and Natalie Glance. Evolutionary games and computer simulations. *Proceedings of the National Academy of Sciences, USA*, 90:7716–7718, August 1993.

[Hin00a] Haye Hinrichsen. Nonequilibrium critical phenomena and phase transitions into absorbing states. *Advances in Physics*, 49:815–958, 2000.

[Hin00b] Haye Hinrichsen. On possible experimental realizations of directed percolation. *Brazilian Journal of Physics*, 30(1):69–82, March 2000.

[Kin83] Wolfgang Kinzel. Directed percolation. In R. Zallen G. Deutscher and J. Adler, editors, *Percolation Structures and Processes*, page 425. Adam Hilger Pub. Co., Bristol, 1983.

[Lou02] Pierre-Yves Louis. *Automates Cellulaires Probabilistes : mesures stationnaires, mesures de Gibbs associées et ergodicité*. PhD thesis, Université des Sciences et Technologies de Lille, September 2002.

[Moo62] Edward F. Moore. Machine models of self-reproduction. *Proceedings of Symposia in Applied Mathematics*, 14:17–33, 1962. (Reprinted in Essays on Cellular Automata, A.W. Burks (ed.), University of Illinois Press, 1970).

[MZ98] Luis G. Morelli and Damian H. Zanette. Synchronization of stochastically coupled cellular automata. *Physical Review E*, pages R8–R11, July 1998.

[ÓdorBS93] Géza Ódor, Nino Boccara, and György Szabó. Phase pransition study of a one-dimensional probabilistic site-exchange cellular automaton. *Physical Review E*, 48(4):3168–3171, 1993.

[ÓdorS96] Géza Ódor and Attila Szolnoki. Directed-percolation conjecture for cellular automata. *Physical Review E*, 53(3):2231–2238, 1996.

[Rou06] Jean-Baptiste Rouquier. Coalescing cellular automata. In ICCS'06 *Proceedings – LNCS 3993*, pages 321–328, 2006.

[RZ02] Andrea Roli and Franco Zambonelli. Emergence of macro spatial structures in dissipative cellular automata. In *Proc. of ACRI2002: Fifth International Conference on Cellular Automata for Research and Industry*, volume 2493 of *Lecture Notes in Computer Science*, pages 144–155. Springer, 2002.

[SdR99] Birgitt Schönfisch and André de Roos. Synchronous and asynchronous updating in cellular automata. *BioSystems*, 51:123–143, 1999.

[Wol84] Stephen Wolfram. Universality and complexity in cellular automata. *Physica D*, 10:1–35, 1984.

The author expresses his acknowledgements to Hugues Berry and Nicolas Paul for their precious help.